ELSEVIER

Biochimica et Biophysica Acta 1416 (1999) 161–175

BIOCHIMICA ET BIOPHYSICA ACTA
BBA

The amphipathic helix concept: length effects on ideally amphipathic $L_iK_j(i=2j)$ peptides to acquire optimal hemolytic activity

Sabine Castano [a], Isabelle Cornut [b], Klaus Büttner [b], J.L Dasseux [b], Jean Dufourcq [a,*]

[a] *Centre de Recherche P. Pascal, CNRS, 33600 Pessac, France*
[b] *Fournier Pharma GmbH, D-69123 Heidelberg-Wieblingen, Germany*

Received 3 June 1998; received in revised form 1 October 1998; accepted 6 November 1998

Abstract

In a minimalist approach to modeling lytic toxins, amphipathic peptides of L_iK_j with $i=2j$ composition and whose length varies from 5 to 22 residues were studied for their ability to induce hemolysis and lipid vesicle leakage. Their sequences were designed to generate ideally amphipathic α helices with a single K residue per putative turn. All the peptides were lytic, their activities varying by more than a factor of 10^3 from the shortest 5-residue-long peptide (5-mer) to the longest 22-mer. However, there was no monotonous increase versus length. The 15-mer was as active as the 22-mer and even more than melittin which is used as standard. Partition coefficients from the buffer to the membrane increased in relation to length up to 12 residues, then weakly decreased to reach a plateau, while they were expected to increase monotonously with peptide length and hydrophobicity as revealed from HPLC retention times. Fluorescence labeling by a dansyl group at the N-terminus, or by a W near the CO-terminus, show that up to 12 residues, the peptides were essentially monomeric while longer peptides strongly aggregated in the solution. Lipid affinity was then controlled by peptide length and was found to be limited by folding and self-association in buffer. The lytic activity resulted both from lipid affinity, which varied by a factor of 20-fold, and from efficiency in disturbing the membrane when bound, the latter steeply and monotonously increasing with length. The 15-residue-long peptide, KLLKLLLKLLLKLLK, had the optimal size for highest lytic activity. The shallow location of the fluorescent labels in the lipids is further evidence for a model of peptides remaining flat at the interface.

Keywords: Hemolytic peptide; Amphipathic $L_iK_j(i=2j)$ peptide; Peptide–lipid interaction; Fluorescence; Self-association

1. Introduction

In the animal world, cytotoxic peptides, whose length generally does not exceed 40 residues, commonly play both offensive and defensive roles against external aggressions. Located in the defense systems of species as various as bacteria (δ-hemolysin), insects (melittin, bombolittin, cecropin), batracians (magainin) or mammalians (defensin), some of them display specific antimicrobial activities like magainins and cecropins [1] while others, like melittin, are lytic without distinction against bacteria or eukaryotic cells such as erythrocytes. All cytotoxic peptides enhance the permeability of the biological membrane by directly disturbing interaction with the lipid matrix [2–4].

To identify some common structural features in order to understand their activity, it has been shown

* Corresponding author. Fax: +33-5-5684-5600;
E-mail: dufourcq@crpp.u-bordeaux.fr

0005-2736/99/$ – see front matter
PII: S0005-2736(98)00219-3

that a positive net charge and a high amphipathic character allow them to adopt amphipathic secondary structures (α-helix or β-sheet) in a lipid environment [2–4]. Generally, basic peptides with strong hemolytic activity have an amphipathic structure [2–5]. Melittin, the most studied and perhaps the most potent member of this family, was initially considered as a peptidic tensid since it has an essentially apolar N-terminal segment of 19 residues followed by a very strongly charged hexapeptide [6]. However, the synthesis of analogs has shown that among the 19 residues of the N-terminus, a few polar and charged residues are mandatory to obtain full activity [7] and the details of the apolar area have little importance [8]. Such requirements for a secondary amphipathic α-helix hold for strongly lytic δ-toxin [9] and magainin [1,4].

To generate the simplest hemolytic amphipathic peptides, the association of only residues L and K is sufficient: 18-residue-long (L,K) peptides, designed to generate ideal α-helical rods (Fig. 1A) with a 1:1 [10] or a 2:1 [11] L/K ratio, are very active. Other attempts to obtain lytic compounds have used a wider variety of residues [12] or have defined a consensus sequence [13]. Peptides longer than 15 residues are always active in inducing both hemolysis and leakage of material trapped inside liposomes as well as in killing bacteria, essentially Gram-positive ones [12]. These peptides are attractive models to understand the mechanism of lysis.

In this paper we investigate the minimal conditions to obtain lytic L,K peptides. By varying their size to the extreme and looking at activities and affinities for simple phospholipidic and natural membranes, we propose that the well established concept of an α-helix spanning the bilayer is not an absolute requirement. The model of helix bundles generating a channel or hole of variable size should be reconsidered. Moreover, peptide hydrophobicity is always the key parameter governing the affinity for membranes, but its increase is limited by peptide solubility in the buffer which can be the major drawback for obtaining large active peptides.

The peptides studied here (Fig. 1B) were systematically labeled by a dansyl group (Dns) at their N-terminal end to monitor their behavior both in solution and in the presence of lipids and membranes. The effects of N-terminal blockade were also estimated. To detect peptide–peptide contacts by fluorescence energy transfer, an analog of the 15-mer was labeled in the C-terminus by a $L_{14} \rightarrow W$ substitution.

2. Materials and methods

2.1. Materials

The peptides were synthesized on solid phase using the base labile Fmoc-protecting group [11] and purified by high-performance liquid chromatography (HPLC) on a CN column eluted with a CH_3CN gradient. The blank and dansylated peptides from 5 to 15 residues and the W containing LK_{15}, namely $LK_{15}(W_{14})$, were provided by Neosystem (Strasbourg, France) as compounds with purity $\geq 97\%$ on HPLC (Table 1).

Egg phosphatidylcholine (EPC) was prepared and purified in the laboratory; it gives a single spot on TLC. All other lipids were from Lipid Products (Nutfield, UK), Tris and Calcein from Sigma, $CoCl_2$ and Triton X-100 from Aldrich-Chemie. All chemicals were the purest available.

2.2. HPLC analysis

To measure the peptide retention times, analytical reverse-phase HPLC was carried out using a C_{18} reverse phase Puropher RP-18 end-capped semi-preparative column (125×4 nm, 5 μm particle size), in conjunction with a Waters millennium HPLC system. Samples, typically 5 μl of either pure MeOH, or 40% CH_3CN/MeOH peptide dilutions at 1 mg/ml, were monitored at 215 nm using a photodiode array Detector 996 variable wavelength spectrophotometer. The column was eluted in 25 min using a linear gradient of 40–100% acetonitrile (CH_3CN) in water.

Longer peptides were analyzed on a Nucleosyl 300-7 CN column (250×8 mm) in conjunction with a Hewlett Packard model 1050 HPLC system sampler. Typically, 25 μl of 50% CH_3CN/H_20 peptide dilutions at 1 mg/ml were monitored at 215 nm. The column was first eluted for 15 min using a 1:1 (v/v) CH_3CN/H_2O mixture, then for 30 min using a linear gradient of 10–70% CH_3CN in water.

A

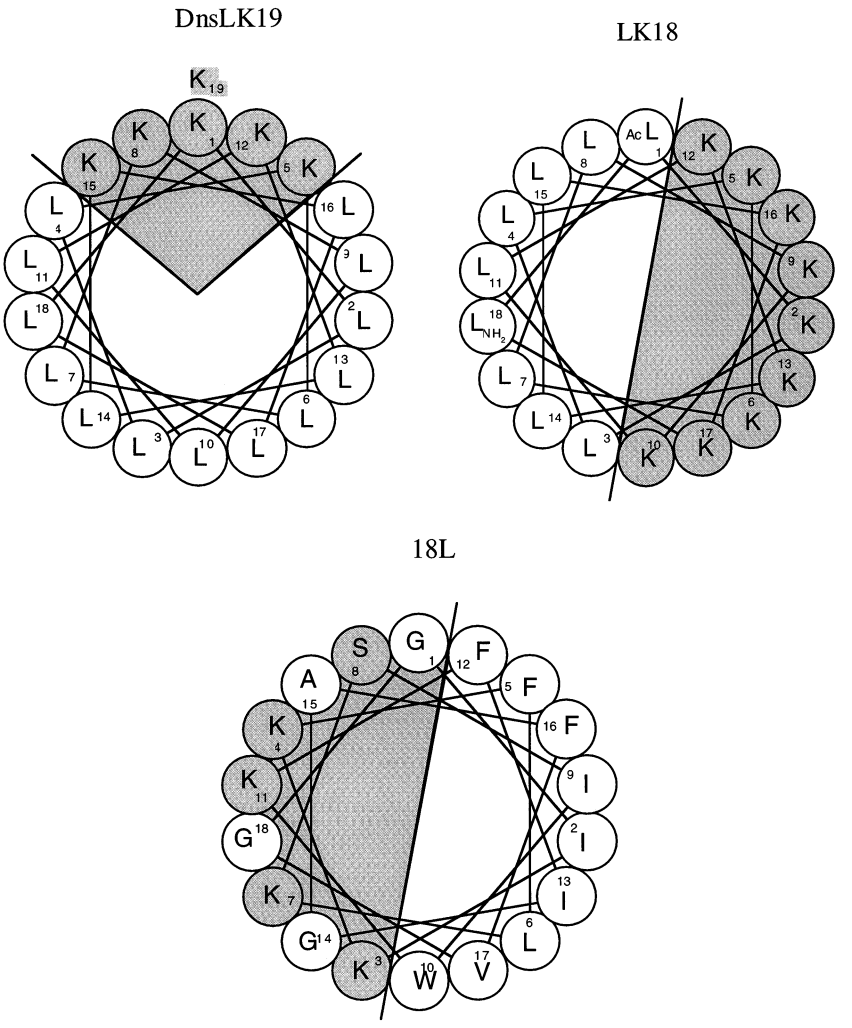

B

Name	Sequence
$DnsLK_5NH_2$	Dns-K L L L K-$CONH_2$
$DnsLK_8$	Dns-K L L L K L L K
$DnsLK_9$	Dns-K L L L K L L L K
$DnsLK_{12}$	Dns-K L L L K L L L K L L K
$DnsLK_{15}$	Dns-K L L K L L L K L L L K L L K
$DnsLK_{19}$	Dns-K L L L K L L K L L L K L L L K L L K
$DnsLK_{22}$	Dns-K L L K L L L K L L K L L L K L L L K L L K
$DnsLK_8NH_2$	Dns-K L L L K L L K-$CONH_2$
$DnsLK_9NH_2$	Dns-K L L L K L L L K-$CONH_2$
$DnsLK_{22}NH_2$	Dns-K L L K L L L K L L K L L L K L L L K L L K-$CONH_2$
ia-$LK_{15}(W_{14})$	K L L K L L L K L L L K L W K
r-$LK_{15}(W_{14})$	L K L L L L K L L K L K L W K

Fig. 1. Sequences and Schiffer–Edmundson's helical wheel representation of the peptides studied. (A) Helical wheel representation of $DnsLK_{19}$ with ($i=2j$) compared to the 18-mers LK_{18}, with ($i=j$) previously studied by Blondelle and Houghten [10] and the 18L consensus sequence proposed by Tytler et al. [13]. (B) Sequences and abbreviations of the L_iK_j ($i=2j$) peptides studied herein.

Table 1
Physical and chemical parameters of the peptides studied

Name	Composition	Molecular weight (g/mol)	Total hydrophobicity	Net charge
$DnsLK_5NH_2$	L3K2	846	−0.61	+2
$DnsLK_8$	L5K3	968.3	−0.65	+2
$DnsLK_9$	L6K3	1081.5	−0.12	+2
$DnsLK_{12}$	L8K4	1436	−0.16	+3
$DnsLK_{15}$	L10K5	1790.5	−0.20	+4
$DnsLK_{19}$	L13K6	2255	+0.29	+5
$DnsLK_{22}$	L15K7	2609	+0.24	+6
(r-, ia-) $LK_{15}(W_{14})$	L9WK5	1863.5	−0.36	+5

Components contained 0.1% TFA and were eluted at a flow rate of 1 ml/min.

2.3. Lipid vesicle preparations

Small unilamellar vesicles (SUVs) used in fluorescence experiments for lipid/peptide interaction were prepared from a lyophilized lipid mixture (EPC–5% cholesterol) hydrated by buffer (20 mM Tris, pH 7.4) at about 5–10 mM. After vortexing at 25°C the dispersions were tip-sonicated under N_2 at constant temperature ($\sim$10°C) for 10 min using a Vibracell 72405 apparatus. This resulted in SUVs as already checked by QELS and gel filtration [14].

Large unilamellar vesicles (LUVs) were used for studies of dye release induced by the peptides. The colyophilized lipid mixture EPC/5% Cholesterol (typically 24 mg) was dispersed by vortexing in 3 ml of buffer containing 0.5 mM of calcein. The suspension was quenched 10 times in liquid nitrogen and heated to room temperature. The solution was then passed approximately 15 times through the polycarbonate filter (∅0.2 μm) of an extruder from Lipex (Vancouver, Canada). After 12 h at 10°C the vesicle suspension was loaded on a short Aca 54 column to separate untrapped dye. The recovered LUVs were kept under N_2 at 10°C. Their size, as estimated by QELS, was about 200 nm. The final lipid concentration was determined by phosphorus analysis [15].

When used for leakage induced by peptides, a few microliters of the LUV suspension were added to 2 ml of buffer at 18°C in a quartz cuvette with magnetic stirring. The fluorescence intensity of calcein excited at 490 nm was monitored at 520 nm for over 20 to 30 min. $CoCl_2$ was added (10 μl corresponding to a final concentration of 0.25 mM) before the peptide to ensure the absence of free calcein fluorescence. Fluorescence intensity was generally reduced by about 10% and was indicative only of the trapped dye. Total leakage was estimated after addition of 10 μl of Trito X-100 at 10% [16].

2.4. Hemolytic assay

Fresh human blood from a healthy O^+ donor was collected on citrate and centrifuged at 980 g for 3 min. The erythrocyte pellet was washed three times in saline buffer (20 mM Tris, 130 mM NaCl, pH 7.4) and resuspended in buffer to obtain 10^7 cells/ml as measured by the absorbance of Hb, ($\varepsilon_{414} = 4.2 \times 10^5$ $M^{-1}\,cm^{-1}$), thus corresponding to an absorbance OD = 2.0.

Each experiment performed on 96-well ELISA plates was done in triplicate (total volume of 100 μl). Several independent runs were performed. The peptide solution was first diluted by addition of a selected variable small volume of peptide stock solution either in MeOH or MeOH/Tris mixture to the required volume of buffer to obtain 90 μl. After $\approx$20 min, 10 μl of erythrocyte suspension was added to all wells. Plates were incubated at 37°C for 30 min and then centrifuged at 1000 rpm for 10 min. The supernatant was recovered and transferred to another 96-well plate to read the absorbance on a Multiscan MS spectrophotometer. Several controls were carried out. When buffer containing no peptides was added, no lysis occurred (0% hemolysis). 100% hemolysis was measured by diluting cells in pure water. Controls containing only the amount of methanol used for the peptide solution proved that MeOH had no effect.

To monitor the kinetics of hemolysis, different

protocols using 1-ml sample assays were carried out. At different incubation times, hemolysis was stopped by chilling the samples at 4°C and measuring the Hb concentration in the supernatant. In another assay, hemolysis was continuously monitored by measuring the light scattering changes at 620 nm after peptide addition [17,18].

2.5. Fluorescence spectroscopy

Fluorescence emission spectra of dansylated and W-containing peptides were obtained on a Fluoromax spectrofluorimeter from Spex and corrected by comparison with a rhodamine spectrum. Spectra of buffer as well as buffer with lipids were subtracted from the sample spectra to eliminate Raman and light scattering. Generally, several runs were averaged. The emission wavelength was calibrated to obtain the maximum emission of *N*-acetyl tryptophan amide at 350 nm. The single residue Dns-K was used as a reference for a probe totally exposed to the solvent.

Fluorescence energy transfer (FET) between the W (donor) of ia-$LK_{15}(W_{14})$ (Fig. 1B) and the Dns (acceptor) of $DnsLK_{15}$ was performed for peptides alone in buffer and for peptides bound to EPC SUVs at $R_i = 60$. FET was quantified by the quenching of the fluorescence intensity of W for a 1:1 donor/acceptor mixture of peptides (6 μM total peptide concentration) compared to an ia-$LK_{15}(W_{14})$ (3 μM) solution in the same conditions by recording the W fluorescence emission spectra (λ_{exc} (W) = 280 nm) in 20 mM Tris, HCl (pH 7.5) buffer at $T = 25$°C. The transfer efficiency, E, was calculated as $E = 100 \times (I_d - I_{da})/I_d$, where I_{da} is the W fluorescence intensity in the presence of Dns, and I_d its intensity in the same conditions but without Dns, measured at 340 nm. Excitation spectra of Dns for the peptide mixture in solution as well as for that of the peptides bound to SUVs were recorded at λ_{em}(Dns) = 506 nm. Appropriate blanks and the spectrum of direct Dns excitation of the dansylated peptide when excited at 280 nm were always subtracted.

The degree of fluorescence polarization, P, was obtained on a SLM 8000 spectrofluorimeter modified to automatically record I_v, I_h alternately. The P values were averaged on seven acquisitions of I_v and I_h measured alternately for 40 s. The fundamental degree of polarization values, P_0, were estimated through changes in the viscosity of the solution, η, by successive glycerol additions and extrapolation of the straight lines of $P^{-1} = f(T/\eta)$ [19].

Temperature, controlled by Peltier devices, was kept at 25°C or 20°C and the solutions stirred with a magnetic device.

Peptide concentrations were estimated from absorbance measurements of the concentrated solutions on a Pye Unicam Philips 8800 spectrophotometer. For dansylated peptides $\varepsilon_{Dns}^{340} = 4640\ M^{-1}\,cm^{-1}$, and for W-containing peptides $\varepsilon_{W}^{280} = 5600\ M^{-1}\,cm^{-1}$ [18]. The peptide amount in the lyophilized powder was known from quantitative amino-acid analysis and accounted for 50% to 65% according to the peptide used.

3. Results

3.1. Design of amphipathic peptides

Peptides were designed to form ideally amphipathic α-helices with the constraint of having a single charged K residue per putative α-helical turn (Fig. 1A). With this assumption, the total hydrophobic moment (μ_H) was calculated using the consensus scale of hydrophobicity [20]. μ_H varied linearly with the peptide length from $\mu_H = 2.4$ to $\mu_H = 9.8$ for the shorter single putative turn of the 5-mer to the 22-mer, respectively. The mean value for the hydrophobic moment per residue, $\mu_{res} \approx 0.43 \pm 0.05$, was almost constant throughout the series and showed quite a high amphipathic character compared to the natural cytotoxins ($\mu_{res} \approx 0.31$ for melittin).

To check for a progressive increase in amphipathicity and hydrophobicity in the peptide series, their affinity for C_{18} chains on reverse phase HPLC has been proposed to reflect their ability to interact with membranes, and it generally parallels their cytotoxic activity [7]. On a water/CH_3CN gradient, all peptides from 5 to 22 residues elute ranking according to their length (Fig. 2, top). Retention time (RT) increased linearly from 1.4 min for the shorter peptide up to RT = 22 min for $DnsLK_{22}$. Being too hydrophobic, $DnsLK_{22}$ was not well separated from $DnsLK_{19}$.

The rather good correlation between RT and μ_H

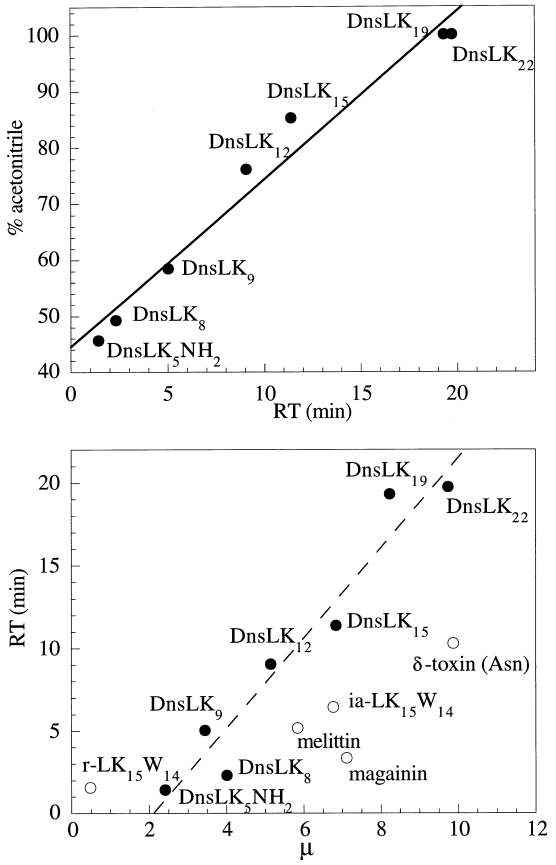

Fig. 2. Hydrophobicity and hydrophobic moment of the $L_iK_j(i=2j)$ peptides studied. (Top) Retention time of the peptides on a C18 column by RP-HPLC on elution with a CH_3CN gradient. Correlation factor $R=0.98$. (Bottom) Plot of the experimental retention times versus the calculated total μ_H values for the peptides of increasing length from 5 to 22 residues. For the sake of comparison, representative data points of natural toxins are added. The solid line represents the best linear regression with a correlation factor $R=0.97$.

(Fig. 2, bottom) means that, in the hydro-organic solvent, the increase in chain parallels the increase in net charge and hydrophobicity (Table 1), as expected from the principles of the peptide design. Thus, these peptides can be used to define how the cytotoxicity varies versus these two parameters.

To check for the effects of blocking the N- and C-termini, several modifications in the peptides were made. As expected, RT values systematically increased upon dansylation and amidation of the C-terminus (Table 2).

The LK_{15} peptide sequence was changed by substitution of the L_{14} into tryptophan (W). This ia-$LK_{15}(W_{14})$ (Fig. 1B) eluted at a lower RT value ($\Delta RT = 0.5$ min) compared to blank LK_{15} (Table 2). A scrambled or random peptide, r-$LK_{15}(W_{14})$ (Fig. 1B), with a more than tenfold reduced μ_H value compared to the ideally amphipathic LK_{15} (0.5 compared to 6.8), was used. It eluted with a very short RT (1.5 min), i.e., rather similarly to the $DnsLK_5NH_2$ peptide (Table 2).

3.2. Hemolytic activity

All peptides from 5 to 22 residues were fully active in hemolysis and displayed quite similar sigmoidal-shaped dose–response curves (Fig. 3). The activity increased versus peptide length, as found previously for a few longer peptides [11]. The shortest $DnsLK_5NH_2$ peptide with both N- and C-terminal ends blocked was still active ($LD_{50} \approx 90$ μM). Increasing the length by three or four residues led to about a tenfold decrease in LD_{50}; the $DnsLK_9$ peptide with both ends blocked was almost as active as the $DnsLK_{12}$. The activity still increased from 12 to 15 residues, the $DnsLK_{15}$ peptide being as active as melittin (Fig. 3). However, the activity decreased for the 18- and 19-mers before recovering a rather similar LD_{50} for $DnsLK_{22}$. Thus, when length increases, hemolytic activity varies non monotonously as a whole by a factor of 10^3.

N-terminal dansylation increased the activity of

Table 2
Influence of N- and C-terminal blockades on the peptide retention times measured on a RP-HPLC column

Dns N-terminus blockage[a]		C-terminus amidation		LK_{15} series	
peptide length	ΔRT (min)	peptide length	ΔRT (min)	peptide length	ΔRT (min)
12	3.9	8	0.9	ia-$LK_{15}W_{14}$	0.5
15	2.6	9	0.7	r-$LK_{15}W_{14}$	−5.3
22	2.2			$DnsLK_{15}$	4.2

Peptide length in number of amino acids. ΔRT = (RT of modified peptide − RT of normal peptide).
[a]On a CN column of HPLC.

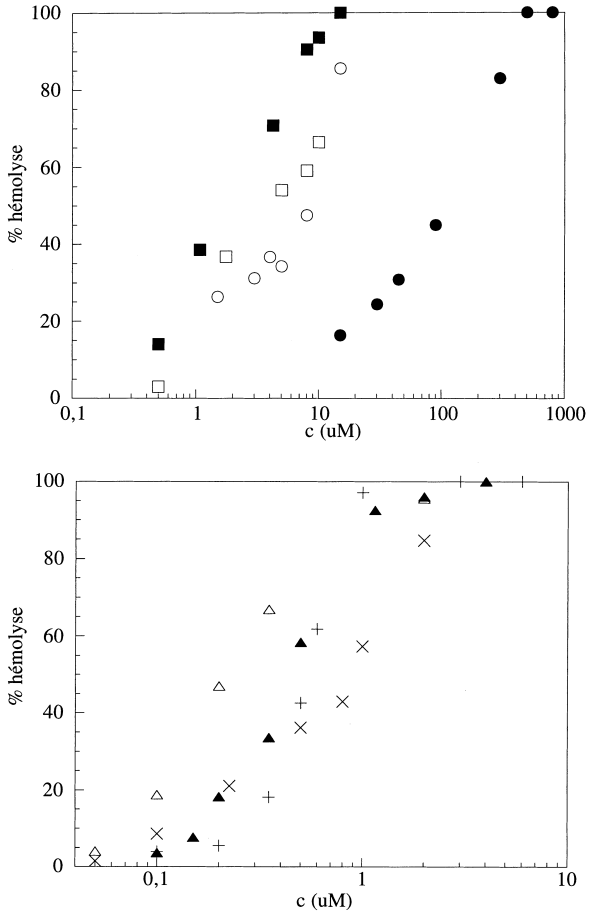

Fig. 3. Dose–response plots of the hemolysis of human red blood cells induced by the Dns $L_iK_j(i=2j)$ peptides. ●, $DnsLK_5NH_2$; ○, $DnsLK_8$; □, $DnsLK_9$; ■, $DnsLK_{12}$; ▲, $DnsLK_{15}$; ×, $DnsLK_{19}$; △, $DnsLK_{22}$; +, melittin. 10^7 cells per ml in 20 mM Tris–HCl, 130 mM NaCl, pH 7.5 buffer after 30 min at 37°C.

the 15-mer by a factor of 2.5-fold ($LD_{50}=0.8$ and 0.3 μM for LK_{15} and $DnsLK_{15}$, respectively). This effect increased when the peptide length decreased. Similarly, the amidation of the C-terminus increased the activity of $DnsLK_9$ and $DnsLK_{22}$ ($LD_{50}=4.5$ and 2.5 μM for free or amidated $DnsLK_9$, respectively, and 0.3 and 0.1 μM for free or amidated $DnsLK_{22}$). L→W_{14} substitution in the ia-$LK_{15}(W_{14})$ did not significantly decrease the activity ($LD_{50}=$ 0.8 μM) while the scrambled r-$LK_{15}(W_{14})$ had a higher LD_{50} value ($LD_{50}=5$ μM).

Finally, whatever the incubation time and protocol, the kinetics of hemolysis performed by direct incubation of the erythrocytes with peptides at the LD_{50} concentrations showed a fast release of hemoglobin and a plateau at $t \geq 30$ min.

3.3. Leakage of a trapped dye from liposomes

The kinetics of calcein leakage at [peptide]= 0.4 μM from zwitterionic EPC LUVs showed that short peptides monotonously increased the leakage, the $DnsLK_8$ being more efficient than the

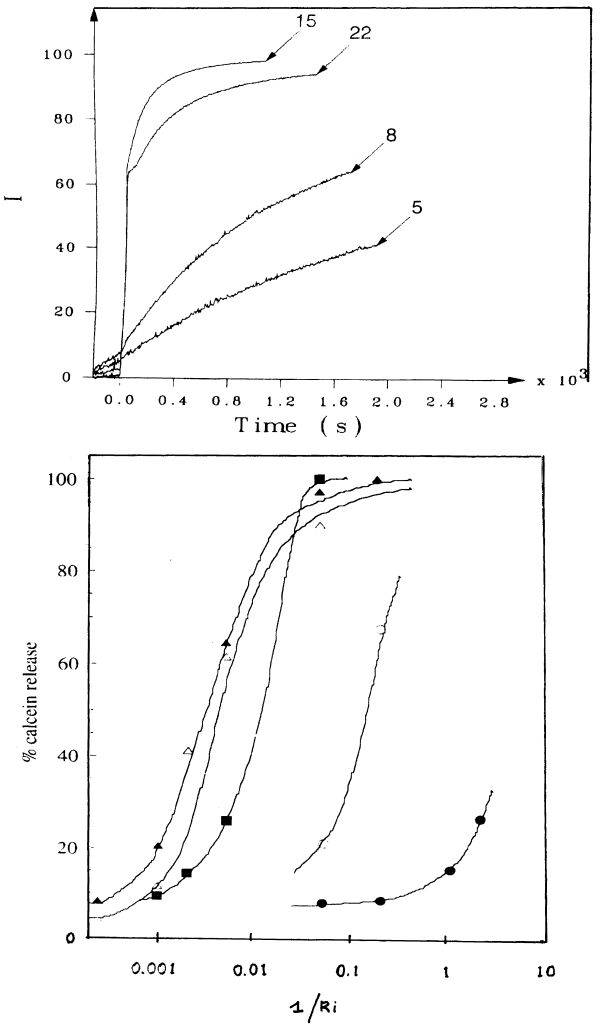

Fig. 4. Leakage of calcein trapped inside LUVs induced by the $DnsL_iK_j(i=2j)$ peptides. (Top) Kinetics of the leakage induced by peptides 5, 8, 22 and 15 residues long from bottom to top, at the same concentration and $R_i=20$. (Bottom) Dose–response plots for the different peptides; the percentage released is defined at 20 min after mixing. ●, $DnsLK_5NH_2$; ○, $DnsLK_8$; ■, $DnsLK_{12}$; ▲, $DnsLK_{15}$; △, $DnsLK_{22}$. LUVs filled with calcein (0.5 mM), [EPC]=8 μM, Tris 20 mM, pH 7.5 buffer, temperature=25°C.

$DnsLK_5NH_2$ (Fig. 4, top). Conversely, the longer peptides induced a large burst followed by a progressive increase up to a maximal release of calcein, a plateau effect being reached within ~20 min. The leakage was dose-dependent and all the peptides induced total release at the highest concentration studied. Values of the concentration needed for 50% of calcein release after 20 min of incubation, C_{50}, show that all the peptides except the shortest permeabilized the vesicles in a sub-micromolar range (Table 3). The leakage ability increased with length up to an optimum for 15 residues. While the 15-mer and the 22-mer displayed almost comparable efficiency, with 50% leakage obtained for R_i about 350, the 19-mer had a ~5-fold lower activity.

3.4. Peptide fluorescence parameters in solution

All the peptides were labeled by a dansyl group (Dns) at the N-terminus of the first K residue. Variations in Dns fluorescence parameters, i.e., wavelength and intensity at the emission maximum (λ_{em}^{max} and I_{em}^{max}, respectively) made it possible to detect local changes in the environment: a decrease in solvent polarity generally induces a hypochrome shift of fluorescence spectra [21].

In relatively apolar solvent methanol, whatever the $DnsL_iK_j(i=2j)$ peptide, $\lambda_{em}^{max} = 523 \pm 1$ nm and $I_{em}^{max} = 1.5 \times 10^6$ indicated a very similar local environment for the Dns (Fig. 5, top) comparable to that obtained for Dns-K. The Dns was therefore totally exposed to the MeOH solvent regardless of the peptide length.

In aqueous Tris buffer, the fluorescence parameters differed significantly with peptide length. For short peptides, namely 5-, 8- and 12-mers (Fig. 5, top), they were similar and quite close to those obtained for Dns-K ($\lambda_{em}^{max} = 549 \pm 1$ nm, $I_{em}^{max} = 0.1 \times 10^6$): the Dns group was totally exposed to the aqueous environment. For longer peptides (≥15 residues), the λ_{em}^{max} strong blue shift and the exaltation of I_{em}^{max} compared to the reference Dns-K (Fig. 5) characterized a Dns burying into a more hydrophobic environment. The Dns fluorescence parameters were quite similar for the 19- and 22-mer, but differed from those of the 15-mer, which are characteristic of the most pronounced burying.

The severe change in the local structure at the N-terminus in buffer when the peptide length increases could a priori be due to either a change in the secondary peptide structure and/or to intermolecular interactions: the longer these amphipathic peptides, the higher their hydrophobicity (Table 1) and their tendency to self-associate by masking apolar residues from water [9].

To detect such effects, Dns polarization degrees (P) were measured both in good solvent methanol and in buffer [22]. In MeOH, very low P values increased weakly and monotonously versus peptide length (Fig. 5, bottom). This indicates fast isotropic motion of the fluorescent group in the time scale of the fluorescence lifetime, i.e., about 10 ns (data not shown). In aqueous buffer, the shorter peptides (5- and 8-mer) still exhibited low polarization degrees, while P steeply increased with peptide length from 8 to 22 residues and reached the fundamental polar-

Table 3
Determination of the intrinsic efficiency of $DnsL_iK_j(i=2j)$ on liposomes ([phospholipids] = 8 μM) and on erythrocytes (equivalent concentration: [phospholipids] = 5 μM)

Peptide	K_p ($\times 10^3$)	On liposomes (LUVs)		On erythrocytes	
		C_{50} (μM)	R_b^{50}	LD_{50} (μM)	R_b^{50}
$DnsLK_5NH_2$	4.0 ± 0.4	39	8	90	3
$DnsLK_8$	8.4 ± 0.8	0.95	170	8.5	18
$DnsLK_{12}$	87.0 ± 8.0	0.11	20.5	2.5	8
$DnsLK_{15}$	50.0 ± 10.0[a]	0.023	1455	0.35	87
$DnsLK_{19}$	50.5 ± 8.0	0.125	267	0.65	46
$DnsLK_{22}$	65.0 ± 8.0	0.023	1142	0.30	94

K_p, partition constant of the peptide between the aqueous phase and the lipid membrane of SUVs (quantitative analysis of the fluorescence data from Fig. 6); C_{50}, concentration of bound peptide at 50% of lysis on liposomes (from data in Fig. 4); LD_{50}, lethal dose on hemolysis (from Fig. 3); R_b^{50}, lipid-to-bound peptide ratio at 50% of lysis either on liposomes or on erythrocytes.
[a] From ia-$LK_{15}W_{14}$ values.

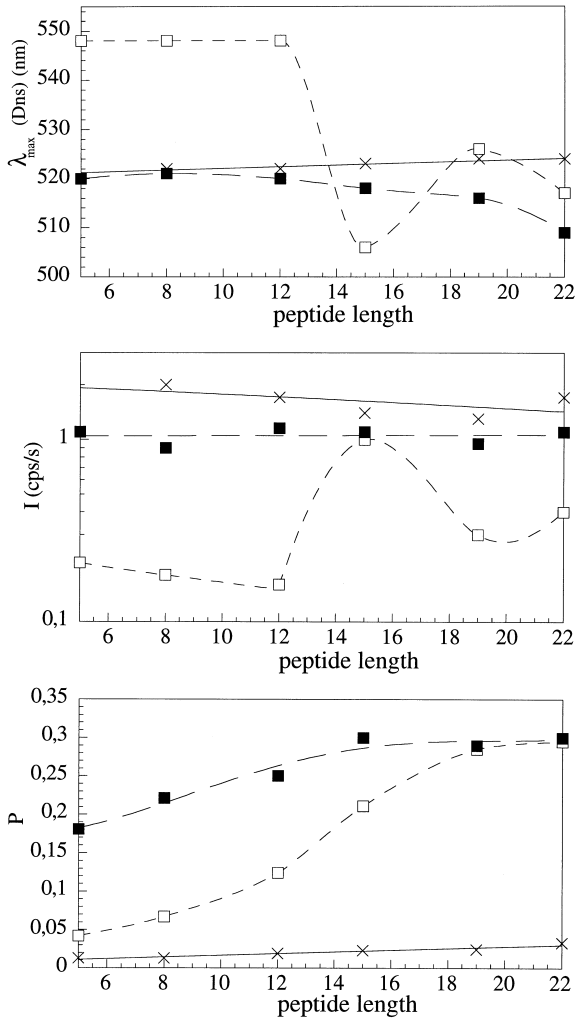

Fig. 5. Changes in the fluorescence parameters of the dansyl group for the labelled $L_iK_j(i=2j)$ peptides versus the peptide length and in different media. (Top) Changes in emission wavelength of the maximum, λ_{max}. (Middle) changes in fluorescence intensity, *I*. (Bottom) changes in polarization degree, *P*. Peptide concentration was always 1.5 μM, $\lambda_{exc}=340$ nm peptides dissolved: ×, in methanol; □, in Tris 20 mM, pH 7.5 buffer; ■, in the same buffer and in the presence of EPC–5% CHOL at $R_i=150$.

ization value, $P_0 \approx 0.3$, determined in pure glycerol (Fig. 5, bottom). The Dns probe was progressively immobilized at the time scale of several tens of ns. This was interpreted as being due to severe self-association.

3.5. Binding of peptides to SUVs as detected by fluorescence: quantitative analysis

Additions of EPC/Chol SUVs at a determined molar ratio, R_i, changed the fluorescence parameters for all the peptides of the series, indicating their binding to the lipids. For peptides shorter than 12 residues, the large blue shift in λ_{em}^{max}(−38 nm) and the fluorescence exaltation (∼6-fold enhanced) in parallel to the drastic increase in *P* (Fig. 5) proved that the Dns of the monomeric-free peptides reached a more hydrophobic environment where the mobility was reduced when the peptides bound to the vesicles. For peptides longer than 19 residues, the weaker blue shift in λ_{em}^{max} (-10 ± 2 nm) and the lower fluorescence exaltation (≅3-fold) (Fig. 5, top and middle) also show the shift of the Dns from an already buried environment in peptide oligomers into an even more hydrophobic one in lipid bilayers. The polarization degrees, constant at $P \approx P_0 \approx 0.3$ throughout the binding process, showed a total lack of motion of the Dns whatever the environment.

The 15-residue-long peptide behaved differently: I_{em}^{max} was weakly modified by lipid additions and λ_{em}^{max} was red-shifted from 505 nm to 515 nm. Therefore, the Dns environment in lipids became less apolar than that observed in the peptide oligomers. In parallel, a *P* increase to P_0 characterized a total Dns immobilization in the lipids.

Whatever their length and state in the buffer, all the peptides exhibited very similar fluorescence parameters in the presence of lipid excess at $R_i=150$, showing a quite comparable Dns local environment in the bound state.

From a double reciprocal plot of I_{em}^{510nm} versus R_i obtained on successive SUV additions up to $R_i \sim 150$, the characteristic change in intensity for totally bound peptides was extrapolated and the fraction of bound peptide (α) defined (Fig. 6). For all the peptides except the 15-mer, the experimental data were analyzed with the simple partition model between two phases: the aqueous one and the lipidic one in vesicles [23]. The partition constant, K_p, defined as the ratio of the peptide concentration in both phases, makes it possible to quantify a relative peptide affinity for each phase.

Log K_p, therefore the affinity for the lipidic phase, increased regularly with peptide length up to 12 residues (Table 3). $DnsLK_5NH_2$ displayed the weaker K_p value (4.5×10^3) which was approximately 2- and 20-fold enhanced when length was increased to 8 then to 12 residues, respectively. When peptides

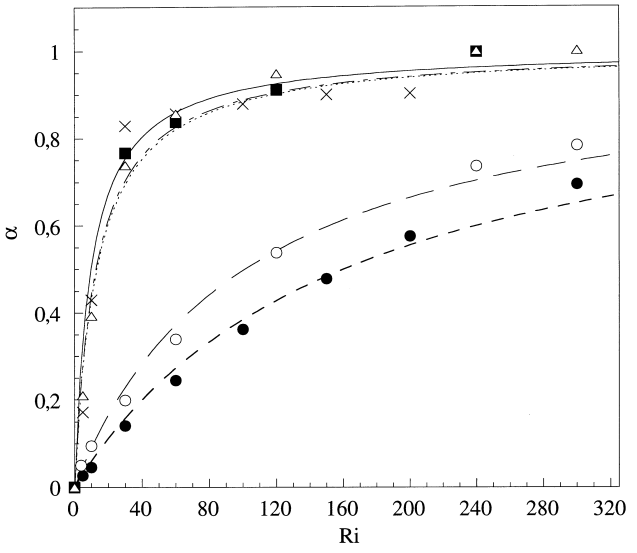

Fig. 6. Quantitative analysis of the interaction of peptides with EPC–5% CHOL vesicles as monitored from fluorescence intensity changes. α is the fraction of bound peptide, R_i the lipid-to-peptide molar ratio. Peptide concentrations were 1.5 μM for Dns LK_8, Dns LK_{12} and $DnsLK_{22}$ and 2 μM for Dns LK_5NH_2 and Dns LK_{19}. Tris 20 mM, pH 7.5 buffer, $T=25°C$. ●, Dns LK_5NH_2; ○, Dns LK_8; ■, Dns LK_{12}; ×, Dns LK_{19}; △, Dns LK_{22}. Lines are calculated best fits according to a simple partition of the peptide with the K_p values reported in Table 3.

were longer than 12 residues, the progressive K_p decrease from $87\pm8\times10^3$ to $50\pm8\times10^3$ and $65\pm8\times10^3$ for the 19- and 22-mer, respectively, showed a complex evolution of lipid affinity with peptide length.

3.6. FET between ia-$LK_{15}(W_{14})$ and $DnsLK_{15}$ in solution and bound to EPC SUVs

Since Dns of the Dns-LK_{15} peptide was not sensitive to lipid binding, ia-$LK_{15}(W_{14})$ was used first to check for the binding to lipids and second to look at FET between W and Dns.

In diluted solution, λ_{em}^{max} of ia-$LK_{15}(W_{14})$ at 348 nm indicated a rather exposed tryptophan residue. When $DnsLK_{15}$ was added at a 1:1 donor/acceptor ratio, the W fluorescence was significantly quenched, $E=18\%$, and the Dns emitted at 506 nm (Fig. 7, top). Furthermore, the Dns excitation spectrum showed a peak at 280 nm due to W excitation (Fig. 7, bottom). This proved the existence of FET from W to Dns in solution.

Increasing the ionic strength favors the formation of oligomers in amphipathic basic peptides [2]. The quenching of the W increased up to 70% at 1 M NaCl, indicating the formation of co-oligomers in agreement with the self-association process observed by fluorescence polarization. By a quantitative measurement of transfer efficiency, a W to Dns mean distance ($R_{W/Dns}$) was estimated by the Förster equation:

$$R_{W/Dns} = R_0(E^{-1}-1)^{1/6}$$

Using $R_0=20$–21 Å [18,24] resulted in 25.8 Å at low

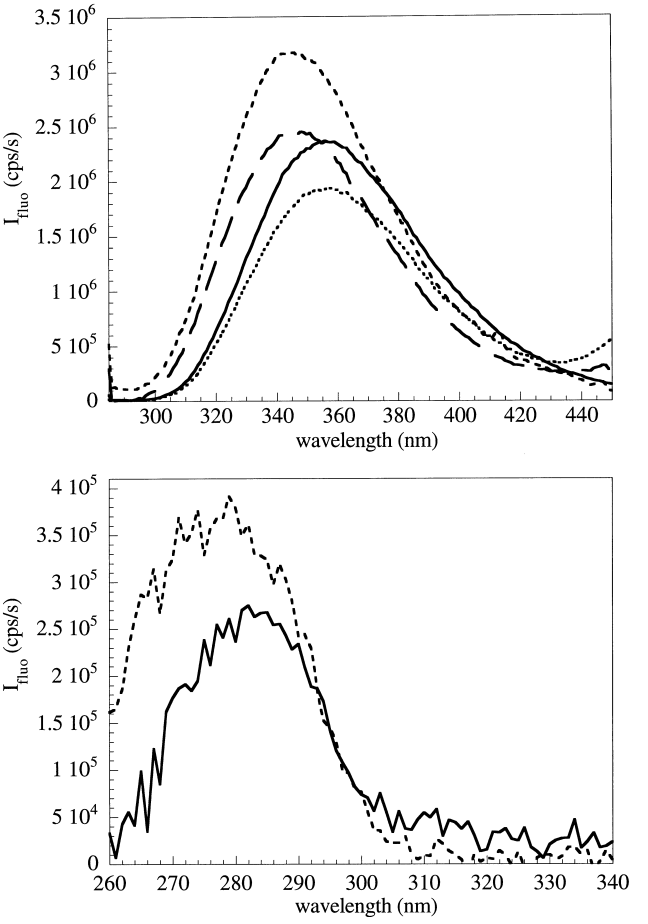

Fig. 7. (Top) Tryptophan fluorescence emission spectra in solution and bound to lipids of ia-$LK_{15}(W_{14})$ and ia-$LK_{15}(W_{14})$/Dns-LK_{15} (1:1) mixture, $\lambda_{exc}=280$ nm. ia-$LK_{15}(W_{14})$ alone: solid line, in solution; dashed line, in the bound state; ia-$LK_{15}(W_{14})$/Dns LK_{15} (1:1) mixture: dotted line, in solution; broad dashed line, in the bound state. (Bottom) Dns excitation spectra of Dns LK_{15} in solution and when bound to EPC SUVs for ia-$LK_{15}(W_{14})$/Dns LK (1:1) mixture, $\lambda_{em}=506$ nm. solid line, in solution; dashed line, in the bound state. [Peptide]=3 μM for each one, 20 mM Tris–HCl, pH=7.5 buffer, $T=25°C$, $R_i=60$.

ionic strength for ia-$LK_{15}(W_{14})$/$DnsLK_{15}$ (1:1) co-oligomers which decreased to 18.2 Å at 1 M NaCl.

EPC SUVs addition to pure ia-$LK_{15}(W_{14})$ shifted the emission maximum by about 10 nm while its intensity increased by 32% (Fig. 7, top). The quantitative monitoring of ia-$LK_{15}W_{14}$ binding to the lipids, as already explained above for Dns peptides, gave $K_p \approx 50 \pm 10 \times 10^3$.

When lipids were added up to $R_i = 60$ to a 1:1 peptide mixture, the λ_{em}^{max} (W) blue-shift of 9 nm (Fig. 7, top) and the concomitant Dns emission red-shift to 521 nm showed that both peptides interacted with the vesicles. Compared to the ia-$LK_{15}W_{14}$ alone in similar binding conditions, the W fluorescence in the 1:1 ia-$LK_{15}(W_{14})$/$DnsLK_{15}$ mixture was quenched (Fig. 7, top). In parallel, the peak at ~280 nm on the Dns excitation spectrum (Fig. 7, bottom) proved a FET from W to Dns for the peptides bound to lipid membranes. In these conditions, the transfer efficiency, $E \approx 22\%$, led to $R_{W/Dns} \approx 25.7$ Å, which again indicates a close proximity of both fluorophores when the peptides are bound to lipids.

4. Discussion

To address the minimal conditions for obtaining lytic peptides, the influence of peptide length was studied for a series of amphipathic $L_iK_j(i = 2j)$ peptides from 5 to 22 residues designed to fold into a putative ideally amphipathic α-helix generating a wide hydrophobic sector (≈260°) (Fig. 1A). The length increase results both in a linear increase in the positive net charge from +2 to +6 and in hydrophobicity (Fig. 2, bottom).

4.1. Lytic activities on cells and liposomes

All the $L_iK_j(i = 2j)$ peptides displayed a strong hemolytic activity (Fig. 3). The shorter peptides (≤12 aa) were more active than the shortest natural 13–14-residue-long mastoparans or crabolins [25], these in turn being 100- to 1000-times less active than $DnsLK_{12}$ and $DnsLK_{15}$. The longer peptides are as or more efficient than natural melittin and the activity of $DnsLK_{22}$ compares to that of the 22-residue-long melittin analog found in frogs [26], despite a higher net positive charge and no sequence homology. A reductionist strategy is therefore potent to generate active compounds, and sophisticated compositions and sequences are not required to obtain efficient lytic compounds.

$L_iK_j(i = 2j)$ can also be compared to other model peptides developed to mimic natural cytotoxins. The lytic 18L peptide [13] (Fig. 1A), proposed as a consensus, is probably as active as our compounds of similar length but does not have any sequence analogy. More interestingly, a series of L_iK_i peptides, i.e., with a 1:1 L/K ratio, studied on hemolytic activity at a single peptide concentration (≈35 μM), shows that peptides shorter than 15 residues are inactive [10]. Our peptides are therefore much more active. Indeed using a single low 0.5 μM concentration proves that activity increases roughly in parallel with peptide length: $DnsLK_{22} \approx 80\% >$ $DnsLK_{15} \approx 60\% >$ $DnsLK_{19} \approx 40\% >$ $DnsLK_{12} \approx 12\% >>$ $DnsLK_9$ and $DnsLK_5NH_2 \approx 0\%$. This totally fits with the parallel increases in activity and hydrophobicity documented for 18-residue-long peptides both by single point K/L substitutions [10] and by systematic broadening of the apolar face angle of putative α-helices from 100° up to 260° by increase of the L content from L/K = 1 up to 2 [27]. In the latter case, the most active compound has the same composition, $L_{13}K_5$, as our $DnsLK_{18}$ peptide [11] despite some subtle differences in their sequences. However, our data show that peptide length is not a critical parameter for activity as long as an optimal hydrophobic-hydrophilic balance is reached.

The first target for the peptides is necessarily the outer leaflet of the erythrocyte membrane, mainly composed of zwitterionic phospholipids (PC, SM, PE). Therefore, the electrically neutral EPC bilayer is a good system to investigate lytic activity. The almost parallel evolution of lytic activities towards erythrocytes and liposomes versus length (Fig. 8) fits with the fact that the hemolytic effect is mainly dictated by hydrophobic interactions of peptides with the neutral lipid matrix as found in KLAL model peptides [28]. So neutral liposomes, which are already accepted as relevant models for natural peptides [29], may be suitable for more quantitative investigations.

For each peptide, the activities on vesicles or cells occur in different concentration ranges: there is a 3- to 20-fold factor between both. This underlines a

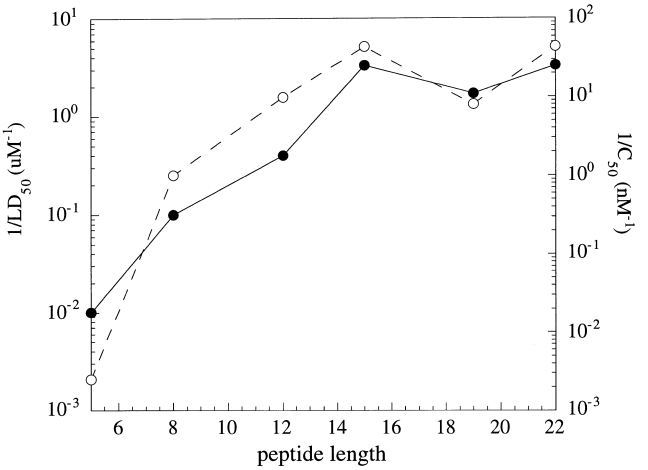

Fig. 8. Comparison of the lytic activity of the Dns$L_iK_j(i=2j)$ peptides towards erythrocytes (●) and EPC LUVs filled with calcein (○). LD_{50} in μM and C_{50} in nM are the peptide concentrations needed to obtain 50% lysis and come from Fig. 3 and Fig. 4, respectively.

large difference in stability between the two models and probably indicates different leakage processes. In the case of cells, hemoglobin leak through a transient opening of the membrane is osmotically sensitive while, in the case of liposomes, the dye escapes through a complex mechanism involving a burst followed by a long lasting period of increased liposome permeability (Fig. 4, top).

Therefore, there is a good correlation between the evolutions of hemolytic activity and leakage efficiency versus length in two different systems. The irregular activity increase, at odds with the linear increase in hydrophobicity versus length and with predictions based on peptide behavior in a good solvent (Fig. 2), may be explained by peculiarities in peptide behavior. For amphipathic peptides, the structure in buffer has to be considered: the longer the peptide, the less it is water-soluble.

4.2. Self-association of the peptides in buffer solution

The biphasic changes of the Dns fluorescence emission parameters show that hydrophobicity governs peptide behavior in buffer when length increases. The shorter peptides (5- to 12-mer), with highly mobile Dns exposed to buffer, are monomeric in the μM range where lytic activity is observed. Peptides longer than 15 residues have both a buried N-terminus and a very long correlation time for rotation, so they form large oligomers whose structures may differ. The FET experiments (Fig. 7) between W and Dns of LK_{15} peptides prove both the close proximity of fluorescent labels and the formation of mixed aggregates. As expected, this self-association process is favored by the ionic strength increase.

This totally agrees with the increase in the self-association tendency when the hydrophobic face angles of the putative α-helices increase from 100° to 260° for 18-residue-long L_iK_j peptides [27]. Such a process occurs for most of the natural cytotoxic peptides which are generally longer [2,9,22,30].

The L_iK_i peptides up to 22 residues previously studied [10] have at most 9–11 L residues per peptide and their high K content is likely to increase the electrostatic repulsion as well as the water solubility. This prevents their self-association in buffer. However, the rather constant activity found for longer peptides [10] is strongly reminiscent of the behavior of the $L_iK_j(i=2j)$ studied herein, probably indicating self-association.

The self-association of peptides longer than 15 residues in buffer also fits with their folding into α-helices detected by CD [11]. Generally, both processes are concomitant; the monomeric amphipathic peptides are unfolded while the secondary amphipathic character induced by folding generates a large apolar surface unstable in buffer and leading to aggregates, often α-helix bundles [9,22,31,32].

Such a self-association in solution modifies the interactions with membranes, leading to a decrease in the hemolytic activity of the $L_iK_j(i=2j)$, as already observed for melittin and δ-toxin [2,33], and explaining the LD_{50} plateau for peptides longer than 15 residues.

4.3. Lipid affinities of the $L_iK_j(i=2j)$ peptides

Binding experiments of the $L_iK_j(i=2j)$ to EPC SUVs documented from the changes of the Dns and W_{14} fluorescence parameters show that all the peptides bind to bilayers in the μM range. The affinity increases in parallel with peptide length from 5 up to 12 residues, but for longer peptides a plateau or even a decrease is observed. Therefore, peptide states in solution have to be taken into account to interpret this unexpected evolution.

Monomeric peptides (≤ 12) partition from an un-

folded state in solution towards the lipid interface where folding occurs to recover the maximal contribution of the hydrophobic effect. The resulting large apolar surface is then buried and stabilizes the peptide in the lipid medium. On the contrary, for self-associated peptides, hydrophobic burying of the L residues in the apolar core of the aggregates is already acquired in solution. So only marginal changes, reflected by weaker or even reverse changes in the Dns fluorescence parameters (Fig. 5), are induced upon binding to lipids, due to a better burying and to the dissociation of the oligomers within the membrane.

As a result, the chain length increase from 5 to 22 residues, i.e., from 3 to 15 L residues, which was expected to 5-fold increase the free energy of binding due to the hydrophobic effect, only results in an 18-fold increase in K_p. Compared to the huge variations of lytic activities from $\approx 2\times 10^3$ factor on liposomes and a ≈ 300 one on erythrocytes, this modest K_p evolution means that hydrophobicity and lipid affinity are not the only parameters modulating lytic activity.

4.4. Intrinsic efficiency of bound peptides

Assuming that the K_p values previously defined for SUVs remain valid for LUVs, the amount of bound peptide and the lipid-to-bound peptide ratio, R_b^{50}, at 50% lysis were calculated. The same hypothesis was made for erythrocytes, as supported by a rather similar affinity for lipids and cell membranes determined on melittin [18]. A relative hierarchy of peptide efficiency was established within the peptide series by comparing the number of each peptide in the bound state required to induce the same consequence on membrane permeability (Table 3). R_b^{50} values varied from 3 to 8 for $DnsLK_5NH_2$ to one peptide for more than one thousand lipids for $DnsLK_{15}$ and $DnsLK_{22}$ (i.e., a single $DnsLK_{15}$ or $DnsLK_{22}$ bound is as efficient as about 50 to 140 shorter peptides, Table 3). Such values are quite large compared to one peptide for a few tens of lipids for 18L [34].

On LUV and erythrocyte systems, the bound peptide concentrations vary similarly (Fig. 9), but there is on the average a factor of 3 to 10 between both scales of efficiency: peptides are more active on model membranes or LUVs are less stable than erythrocyte cells. In general, the required amount of bound peptide for 50% of lysis decreases when the length increases, i.e., the intrinsic efficiency of peptides increases. Therefore, hydrophobicity and net charge seem to drive efficiency when the peptide is bound.

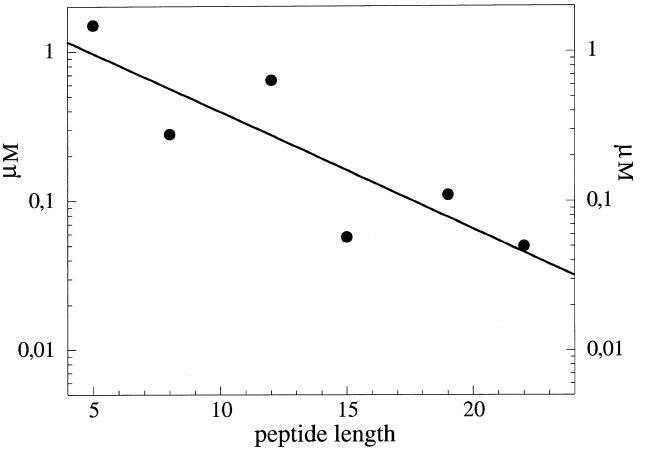

Fig. 9. Evolution of the membrane-bound peptide concentrations required for 50% hemolysis versus peptide length for the $DnsL_iK_j(i=2j)$ series (on erythrocytes at LD_{50} (10^7 cells/ml, 37°C)).

At odds with a regular increase in efficiency versus length, $DnsLK_{12}$ and $DnsLK_{19}$ efficiencies are weaker than expected (Table 3, Fig. 9). This again suggests that the lytic activity should be modulated by parameters other than hydrophobicity and net charge, such as the peptide structure and/or the orientation in the membranes.

4.5. Location of the peptides when bound to the bilayer

Even though the aim of the present work was not to address the problem of the structure of peptides, which will be presented elsewhere [42], the fluorescence data on labeled peptides point to make some proposals concerning their location within the bilayers.

In the lipid bound state, all the peptides display very similar Dns fluorescence parameters (Fig. 5) reflecting a similar location of their Dns group. A plot of Dns λ_{em}^{max} versus the dielectric constant of solvent, ε (data not shown) makes it possible to estimate a mean value $\varepsilon = 25 \pm 5$ for the Dns environment, so Dns is partially buried in an interfacial position. Rather similar locations have been found for Dns

covalently bound to Q_{25}melittin interacting with lecithin vesicles [18], to the polar head group of PE [35] or to the aliphatic chains of lecithins [36].

Similar solvatochromic effects on W fluorescence can be used to locate W_{14} from ia-$LK_{15}(W_{14})$ at $\lambda_{em}^{max} \approx 330$ nm. This value is similar to those of W_{19} of melittin [37], and of W_9 located in the apolar face of the α-helix of a melittin analog [17]. Both for δ-toxin and its analogs bound to PC [38] and for 18-residue-long L_iS_i ideally amphipathic α-helical channel-forming peptides [39], it has been shown that W has an emission maximum at about 342 nm when it substitutes residues on the polar face, while it has an emission between 330 ± 5nm when it substitutes residues on the apolar face embedded in the lipids. Thus, the W residue of ia-$LK_{15}W_{14}$ 'senses' an apolar medium which could correspond to less than 5 Å in the acyl chains.

Further work will be necessary to properly address the location of the fluorophores within the bilayer (see for instance [40]), but for the 15-residue-long peptide, both N- and C-terminus located fluorescent probes are not deeply embedded within the bilayer. Since it adopts an α-helix structure [11,42], the peptide is too short to be transmembranous, so this can not optimize hydrophobic–hydrophilic interactions due to the high K content. Therefore the peptide will lie with its helix axis parallel to the interface, which fits with conclusions from an in situ study by polarization-modulated Fourier transform infrared spectroscopy in a DMPC monolayer at the air–water interface [41,42].

The FET between W_{14} and Dns fluorophores documented herein for the two LK_{15} analogs proves peptide–peptide contacts in the concentration range of lysis. A more systematic study is necessary to know if such a proximity results from favored peptide–peptide interactions or, more likely, from a random distribution of peptides in the membrane plane at a sufficient concentration to set up close contacts.

The fact that peptides with a contiguous single file of K residues regularly distributed along the peptide are even more active than the less charged natural compounds reinforces the idea that all K should remain at the interface, and that this is the genuine active orientation required for lysis. If so, this rules out most of the complex models based on differences in depth of embedding, wedge effects or upon tiny differences due to kinks in the helices. Such a conclusion also fits with the real need for a K_7 residue in melittin [43] and with the fact that for amphipathic histidine-rich peptides, only drastic pH changes resulting in the total loss of net charge allow the reorientation of significant amounts of the peptide from flat to perpendicular to the interface [44].

Lysis may be primarily due to peptides flatly oriented on the outer leaflet of cell membranes. Such a proposal fits well with the schema proposed for different lytic peptides like δ-toxin [45], melittin [2,46] and dermaseptins [47], regardless of whether it is called 'raft' or 'carpet' [48]. By such an asymmetric disturbance, peptide clusters or domains may then destabilize the membrane and induce permeabilization. The constraint relaxation can allow the peptide to span and/or to cross the membrane to equilibrate in/out concentrations, and/or the lipids to flip-flop and decrease the surface excess of the outer layer.

Acknowledgements

We are pleased to acknowledge Wilfrid Néri for his efficient help both in purification and characterization of some peptides by HPLC and in performing hemolytic assays. Dr. Roland Bernon and Pascal Merzeau are acknowledged for developing the full automatization of the SLM 8000 spectrometer. This work was supported by the CNRS program GDR 790 and by a Fournier Pharma – CNRS contract.

References

[1] M. Zasloff, B. Martin, H.C. Chen, Proc. Natl. Acad. Sci. U.S.A. 85 (1988) 910–913.
[2] I. Cornut, E. Thiaudière, J. Dufourcq, in: R.M. Epand (Ed.), The Amphipathic Helix, CRC Press, Boca Raton, FL, 1993, pp. 173–219.
[3] G. Saberwal, R. Nagaraj, Biochim. Biophys. Acta 1197 (1994) 109–131.
[4] W.L. Maloy, U.P. Kari, Biopolymers 37 (1995) 105–122.
[5] R.M. Kini, H.J. Evans, Int. J. Pept. Protein Res. 34 (1989) 277–286.
[6] E. Habermann, Science 177 (1972) 314–322.
[7] S.E. Blondelle, R.A. Houghten, Biochemistry 30 (1991) 4671–4675.
[8] W.F. De Grado, F.J. Kézdy, E.T. Kaiser, J. Am. Chem. Soc. 103 (1981) 679–681.

[9] E. Thiaudière, O. Siffert, J.C. Talbot, J.E. Alouf, J. Dufourcq, Eur. J. Biochem. 195 (1991) 203–213.
[10] S.E. Blondelle, R.A. Houghten, Biochemistry 31 (1992) 12688–12694.
[11] I. Cornut, K. Büttner, J.L. Dasseux, J. Dufourcq, FEBS Lett. 349 (1994) 29–33.
[12] S. Lee, H. Mihara, H. Aoyagi, T. Kato, N. Izumiya, N. Yamasaki, Biochim. Biophys. Acta 862 (1986) 211–219.
[13] E.W. Tytler, J.P. Segrest, R.M. Epand, S.Q. Nie, R.F. Epand, V.K. Mishra, Y.V. Venkatachalapathi, G.M. Anantharamaiah, J. Biol. Chem. 268 (1993) 22112–22118.
[14] J. Dufourcq, J.F. Faucon, G. Fourche, J.L. Dasseux, M. Le Maire, T. Gulik-Krzywicki, Biochim. Biophys. Acta 859 (1986) 33–48.
[15] B.N. Ames, Methods Enzymol. 8 (1966) 115–118.
[16] N. Oku, D.A. Kendall, R.C. Mac Donald, Biochim. Biophys. Acta 691 (1982) 3332–3340.
[17] A.J. Weaver, M.D. Kemple, J.W. Brauner, R. Mendelsohn, F.G. Prendergast, Biochemistry 31 (1992) 1301–1313.
[18] E. Perez-Paya, J. Dufourcq, L. Braco, C. Abad, Biochim. Biophys. Acta 1323 (1997) 223–236.
[19] J.C. Talbot, J. Lalanne, J.P. Faucon, J. Dufourcq, Biochim. Biophys. Acta 689 (1982) 106–112.
[20] D. Eisenberg, Annu. Rev. Biochem. 53 (1984) 595–623.
[21] J.R. Lakowicz (Ed.), Principles of Fluorescence Spectroscopy, Plenum Press, New York, 1983.
[22] J.F. Faucon, J. Dufourcq, C. Lussan, FEBS Lett. 102 (1979) 187–190.
[23] G. Schwarz, G. Beschiaschvili, Biochim. Biophys. Acta 979 (1989) 82–90.
[24] J.R. Lakowicz, I. Gryczynski, G. Laczko, W. Wiczk, M.L. Johnson, Protein Sci. 3 (1994) 628–637.
[25] A. Argolias, J.J. Pisano, J. Biol. Chem. 259 (1984) 10106–10111.
[26] M. Simmaco, G. Mignogna, S. Canofeni, R. Micle, M.L. Mangoni, D. Barra, Eur. J. Biochem. 242 (1996) 788–792.
[27] T. Kiyota, S. Lee, G.V. Sugihara, Biochemistry 35 (1996) 13196–13204.
[28] M. Dathe, T. Wieprecht, H. Nikolenko, L. Handel, M.L. Maloy, D.L. Mc Donald, M. Beyermann, M. Bienert, FEBS Lett. 403 (1997) 208–212.
[29] K. Matsusaki, O. Murase, N. Fuji, K. Miyajima, Biochemistry 34 (1995) 6526–6528.
[30] E. Bairaktari, D.F. Mierke, S. Mammi, E. Peggion, Biochemistry 29 (1990) 10097–10102.
[31] C.E. Dempsey, Biochim. Biophys. Acta 1031 (1990) 143–161.
[32] R. Epand, Y. Shai, J.P. Segrest, G.M. Anantharamaiah, Biopolymers 37 (1995) 319–338.
[33] R.C. Hider, F. Khader, A.S. Tatham, Biochim. Biophys. Acta 728 (1983) 206–212.
[34] I.V. Polozov, A.I. Polozova, E.M. Tytler, G.M. Anantharamaiah, J.P. Segrest, G.A. Woolley, R.M. Epand, Biochemistry 36 (1997) 9237–9245.
[35] E. Schechter, T.R.A. Gulik-Krzywicki, C. Gros, Biochim. Biophys. Acta 241 (1971) 431–442.
[36] D. Bartlett, M. Glaser, R. Welti, Biochim. Biophys. Acta 1328 (1997) 48–54.
[37] J. Dufourcq, J.F. Faucon, Biochim. Biophys. Acta 467 (1977) 1–11.
[38] J.E. Alouf, J. Dufourcq, O. Siffert, E. Thiaudière, C. Geoffroy, Eur. J. Biochem. 183 (1989) 381–390.
[39] L.A. Chung, J.D. Lear, W.F. De Grado, Biochemistry 31 (1992) 6608–6616.
[40] A.S. Ladokhin, P.W. Holloway, Biophys. J. 69 (1995) 506–517.
[41] I. Cornut, B. Desbat, J.M. Turlet, J. Dufourcq, Biophys. J. 70 (1996) 305–312.
[42] S. Castano, B. Desbat, M. Laguerre, J. Dufourcq, Biochim. Biophys. Acta 1416 (1999) 176–194.
[43] E. Perez-Paya, R.A. Houghten, S. Blondelle, J. Biol. Chem. 270 (1995) 1048–1056.
[44] B. Bechinger, J. Mol. Biol. 263 (1996) 768–775.
[45] G. Raghunathan, P. Seetharamulu, B.R. Brooks, H.R. Guy, Proteins 8 (1990) 213–225.
[46] T.C. Terwilliger, D. Eisenberg, J. Biol. Chem. 257 (1982) 6010–6022.
[47] Y. Pouny, D. Rapaport, A. Mor, P. Nicolas, Y. Shai, Biochemistry 31 (1992) 12416–12423.
[48] Y. Shai, Trends Biochem. Sci. 20 (1995) 460–464.